This paper is available on line at http://www.mcponline.org

Trypanosoma brucei Mitochondrial Respiratome: Composition and Organization in Procyclic Form*

Nathalie Acestor‡, Alena Zíková‡§**, Rachel A. Dalley‡, Atashi Anupama‡, Aswini K. Panigrahi‡¶, and Kenneth D. Stuart‡‖**

The mitochondrial respiratory chain is comprised of four different protein complexes (I–IV), which are responsible for electron transport and generation of proton gradient in the mitochondrial intermembrane space. This proton gradient is then used by F_oF_1-ATP synthase (complex V) to produce ATP by oxidative phosphorylation. In this study, the respiratory complexes I, II, and III were affinity purified from *Trypanosoma brucei* procyclic form cells and their composition was determined by mass spectrometry. The results along with those that we previously reported for complexes IV and V showed that the respiratome of *Trypanosoma* is divergent because many of its proteins are unique to this group of organisms. The studies also identified two mitochondrial subunit proteins of respiratory complex IV that are encoded by edited RNAs. Proteomics data from analyses of complexes purified using numerous tagged component proteins in each of the five complexes were used to generate the first predicted protein-protein interaction network of the *Trypanosoma brucei* respiratory chain. These results provide the first comprehensive insight into the unique composition of the respiratory complexes in *Trypanosoma brucei*, an early diverged eukaryotic pathogen. ***Molecular & Cellular Proteomics 10: 10.1074/mcp.M110.006908, 1–14, 2011.***

Mitochondria are dynamic organelles essential for cellular life, death, and differentiation of virtually every eukaryotic cell. They house systems for energy production through oxidative phosphorylation, synthesis of key metabolites, and iron-sulfur cluster assembly. The oxidative phoshorylation system of eukaryotic mitochondria comprises five major complexes located in the mitochondrial (mt)[1] inner membrane, and often abbreviated as mt complexes I–V. The redox energy of the substrates NADH and succinate is first converted into an electrochemical proton potential across the inner mt membrane by respiratory complexes I (NADH:ubiquinone reductase), II (SDH, succinate:ubiquinone reductase), III (bc_1, ubiquinone:cytochrome *c* reductase), and IV (cytochrome *c* oxidase). The electrochemical proton potential is then used by complex V (F_oF_1-ATP synthase) to synthesize ATP from ADP and inorganic phosphate, a mechanism that has essentially remained unchanged from bacteria to human (1). However, parasitic organisms have exploited unique energy metabolic pathways by adapting to their natural host habitats (2). Indeed, the respiratory systems of parasites typically show greater diversity in electron transfer pathways than those of their host, and *Trypanosoma brucei* is no exception to this rule (3).

T. brucei, the causative agent of human African trypanosomiasis (HAT), or sleeping sickness, is a blood-borne pathogenic parasite transmitted by tsetse flies. It has a complex life cycle that alternates between the bloodstream forms (BF) in the mammalian host and several stages in the insect vector starting with the procyclic form (PF) in the midgut. During *T. brucei* differentiation between the distinct life-cycle stages, the mitochondrion undergoes morphological and functional changes, and the parasite switches its energy metabolism from amino acid to glucose oxidation (4). BF cells, which live in sugar-rich environment, use energy metabolism predominantly through the glycolytic pathway (5). They contain no cytochrome-mediated respiratory chain and they possess a unique electron transport chain in the mitochondria, the glycerol-3-phosphate dehydrogenase and the salicyl hydroxamic acid (SHAM)-sensitive alternative oxidase, which is known as the trypanosome alternative oxidase (TAO) (6). Despite the absence of complete cytochrome-containing complexes III and IV in BF trypanosomes, a mt membrane potential is maintained and involves the hydrolytic activity of the F_oF_1-ATP synthase complex (7). Conversely, PF cells are dependent on the cytochrome-containing respiratory chain and ATP

From the ‡Seattle Biomedical Research Institute, Seattle, WA 98109, §Biology Center, Institute of Parasitology, University of South Bohemia, České Budějovice, Czech Republic, ¶King Abdullah University of Science and Technology, Thuwal, Kingdom of Saudi Arabia

Received December 2, 2010, and in revised form, May 18, 2011

Published, MCP Papers in Press, May 24, 2011, DOI 10.1074/mcp.M110.006908

[1] The abbreviations used are: mt, mitochondrial; BNE, Blue Native Electrophoresis; hrCNE, high resolution Clear Native Electrophoresis; mAb, monoclonal antibody; LC-MS/MS, liquid chromatography tandem mass spectrometry; OGDC, 2-oxoglutarate dehydrogenase complex; PF, procyclic form; TAP, tandem affinity purification; *T. brucei*, *Trypanosoma brucei*.

generated by conventional function of the F_oF_1-ATP synthase complex for their energy production (8, 9). The branched electron-transport chain contains four complexes that donate electrons to the ubiquinone pool, two NADH:ubiquinone oxidoreductases (complex I and a rotenone-insensitive enzyme), complex II, and glycerol-3-phosphate dehydrogenase. Reduced ubiquinol can be reoxidized by the transfer of electron to either the TAO, which does not translocate protons, or to the cytochrome-containing complexes III and IV that produce a proton motive force by translocation of protons and thus create essential membrane potential (10).

Although the *T. brucei* genome has been sequenced (11), little information is available on the subunit composition of mt complexes I–V based on similarity searches. However, some respiratory complexes have been partially characterized in other trypanosomatids such as *Crithidia fasciculata*, *T. cruzi*, and *Leishmania tarentolae* (12–15). In recent studies, we have determined the protein composition of complexes IV and V, and part of complex I purified from mitochondria of *T. brucei* PF cells (8, 16, 17, 25). These analyses revealed the uniqueness of respiratory complexes in trypanosomes, where large numbers of component proteins have no homologs outside of the Kinetoplastida.

In this study, we focus on the comprehensive characterization of all respiratory complexes in *T. brucei*, collectively termed the respiratome. We report the composition of complexes II and III from PF cells, and extend the characterization of complex I by identifying additional protein constituents. This included the identification of two subunits of the respiratory complex IV, both encoded by mt edited RNAs. We also present a predicted protein-protein interaction network of the respiratome, which was generated using proteomics data collected from numerous tagged proteins in each of the complexes I–V. Our results provide a comprehensive insight into the unique composition of the respiratory complexes in one of the life-cycle stages of *T. brucei*.

EXPERIMENTAL PROCEDURES

Cell Growth—*T. brucei* PF cells IsTat 1.7a were grown *in vitro* at 27 °C in SDM-79 media containing hemin (7.5 mg/ml) and 10% (v/v) fetal bovine serum to a density of 1–2 $\times$ 10^7 cells/ml. PF *T. brucei* strain 29.13 (18), which contains integrated genes for T7 polymerase and the tetracycline repressor, was grown in the presence of G418 (15 μg/ml) and hygromycin (25 μg/ml). The cells were harvested by centrifugation at 6000 $\times$ *g* for 10 min at 4 °C.

Tandem Affinity Purification (TAP)-tagged Cell Lines—To create constructs for the inducible expression of TAP tagged proteins in *T. brucei*, the open reading frames of interest were PCR amplified from the genomic DNA of *T. brucei* strain Lister 427. A detailed list of all tagged proteins and primers used to amplify the selected open reading frames is provided in the supplemental material. The PCR products were cloned into pGEM-T easy vector, digested with BamHI or BglII and HindIII enzymes, and ligated into the pLEW79-MHT vector (19, 20). The plasmids were linearized with NotI enzyme, transfected into PF *T. brucei* 29.13 cell line, phleomycin-resistant clones were selected, and checked for tetracycline-regulated expression. The transgenic PF cell lines expressing a TAP-tagged protein were supplemented with 2.5 μg/ml phleomycin.

Sample Preparation for Native Electrophoresis—Mt vesicles were isolated from IsTat 1.7a cells by hypotonic lysis followed by density gradient flotation in 20–35% linear Percoll gradients (21). The enriched vesicles were solubilized by adding *n*-dodecyl-β-D-maltoside corresponding to *n*-dodecyl-β-D-maltoside/protein ratio of 2 (g/g) and incubated on ice for 30 min. Insoluble material was removed by centrifugation at full speed in a microcentrifuge for 30 min at 4 °C.

Blue Native Electrophoresis (BNE) and High-resolution Clear Native Electrophoresis (hrCNE)—For BNE, 100 μg of mt lysate was supplemented with a 5% (w/v) stock solution of Coomassie Blue G-250 in 500 mM 6-aminohexanoic acid and analyzed on a 3–12% acrylamide gradient gel (8) using 50 mM Tricine, 15 mM Bis-Tris, pH 7.0, 0.02% Coomassie Blue G-250 as cathode buffer, and 50 mM Bis-Tris, pH 7.0 as anode buffer. For hrCNE (22), 100 μg of mt lysate was supplemented with 50% glycerol, 0.1% Ponceau S, and analyzed on a 4–13% acrylamide gradient gel using 50 mM Tricine, 7.5 mM imidazole, pH 7.0, 0.05% deoxycholate as cathode buffer, and 25 mM imidazole, pH 7.0 as anode buffer. All the native gels were run at 4°C at 100 V until the dye marker approached the gel front.

In-gel Catalytic Activity Assays—Following electrophoresis, complex I–V bands were visualized by activity staining as previously described (22). Briefly, to visualize complex I activity, the gel was incubated in 100 mM Tris-HCl, 0.1 mg/ml NADH, and 2.5 mg/ml nitrotetrazolium blue, pH 7.4. To visualize complex II activity, the gel was incubated in 50 mM phosphate buffer, 20 mM sodium succinate, 0.2 mM phenazine methasulfate, 2.5 mg/ml nitrotetrazolium blue, pH 7.4. For complex III, the gel was incubated in 50 mM phosphate buffer, pH 7.2 and 0.05% 3,3′-diaminobenzidine tetrahydrochloride; and the specificity of the reaction was demonstrated using 2 mM antimycin A. For complex IV, the gel was incubated in 50 mM phosphate buffer, pH 7.2, 0.05% 3,3′-diaminobenzidine tetrahydrochloride and 50 μM horse heart cytochrome *c*. Reactions were carried out at room temperature by slow agitation overnight and stopped by fixing the gels in 45% methanol and 10% acetic acid. Complex V was visualized as previously reported (8).

Native Western Blot Analysis for Complex I and III—Following electrophoresis, the native gels were transferred onto an Immobilon membrane overnight at 20 V at 4°C. The membranes were then blocked with Odyssey® Blocking Buffer, probed with mAb52 (1:10), which recognize a native epitope of subcomplex Iα (16) or with rabbit polyclonal antibodies against *T. brucei* apocytochrome c_1 (apoc_1) (1:1000) (23) to detect complex III. IRDye680 conjugated goat anti-rabbit (LiCor 926–32221) and IRDye800 conjugated goat anti-mouse (Rockland 610–132-121) were used as secondary antibodies at 1:15,000. Protein signal was detected by Odyssey™ Infrared Imaging System (LI-COR Biosciences, Lincoln, NE) using one-color fluorescence detection at 700 or 800 nm and analyzed with Odyssey version 3.0 software.

Tandem Affinity Purification of Tagged Complexes—TAP-tagged proteins were expressed by induction with tetracycline (100 ng/ml of culture) for 48 h and 500 ml of cells were harvested by centrifugation at a density of ~2 $\times$ 10^7 cells/ml. Tagged complexes were purified from cell lysates by two methods as previously described (8, 16). Briefly, in method 1 (M1) the harvested cells were lysed by 1% Triton-X 100 and the tagged complexes were isolated by IgG affinity chromatography. The bound complexes were eluted by TEV protease cleavage and fractionated on 10–30% glycerol gradients by centrifugation for 5 h at 38,000 rpm at 4 °C in Beckman Ultracentrifuge (SW40 Ti swinging bucket rotor). The sedimentation profiles of the tagged complexes were monitored by Western blot analyses using anti-His_6 mAb. Peak reactive fractions were pooled and further purified by calmodulin affinity chromatography. In method 2, the tagged

complexes were purified from cells lysed with 0.25% Nonidet P-40, cleared by low speed centrifugation and the supernatant was further treated with 1.25% Nonidet P-40 and cleared by high speed centrifugation. The tagged complexes were isolated by sequential IgG and calmodulin affinity columns.

Immunofluorescence Assay—Subcellular localizations of the expressed tagged proteins within the cell were determined by immunofluorescent assay using anti *c*-myc antibody (Sigma) as described (16). Colocalization analysis was performed using mAb 78 against mt heat shock protein 70 (16) coupled with Texas® Red-X conjugated secondary antibody (Invitrogen).

Protein Identification—We prepared and analyzed the samples by gel-based and gel-free approaches as described previously by us (16, 24, 25). Briefly, proteins in gel pieces were reduced with 10 mM dithiotreitol at 56 °C for 30 min, and alkylated with 55 mM iodoacetamide at room temperature for 45 min, and digested with sequencing-grade modified trypsin (Promega, Madison, WI) at 37 °C overnight; and the resulting peptides were extracted. The TAP tag-purified protein samples were precipitated with 6 volumes of acetone, and the proteins were denatured with 8 M urea, 1 mM dithiotreitol; diluted 1:4, and digested in-solution with trypsin. The resulting peptides were purified using C_{18} beads (Magnetic Dynabeads RPC18, Invitrogen). The peptides from gel pieces or complex mixtures were fractionated by nanoflow liquid chromatography using a 10-cm-long × 75-μm-inner diameter C_{18} capillary column and analyzed on line by electrospray ionization tandem mass spectrometry using a linear trap quadrupole mass spectrometer (Thermo Electron). The bound peptides were eluted from the C_{18} column at a flow rate of 200 nl/min with a 45-min linear gradient of 5–40% acetonitrile in 0.4% acetic acid followed by a 5-min linear gradient of 40–80% acetonitrile in 0.4% acetic acid.

Xcalibur 1.4 SR1 version software was used to collect MS data, and the mass range for the MS scan was *m/z* 400–1400. The tandem MS (MS/MS) data of the five most intense ions were collected sequentially following each MS scan using the dynamic exclusion parameter, where a specific ion was sequenced only twice and was excluded from the list for 45 s. The MS data were analyzed against *T. brucei* v4.0 predicted protein sequence database (11), which contains 9211 protein entries and additionally 18 predicted protein sequence from mt encoded edited and unedited RNAs, and bovine serum albumin, immunoglobulin heavy and light chains and keratin sequences. The peak list generation and search against database were carried out using SEQUEST module of Bioworks 3.1, cluster version SR1 (parameters: molecular weight range, 400–3500; mass tolerance, 1.0 Da; group scan, 25; minimum ion count, 15; no enzyme was specified during the search; no fixed modification was set for any of the amino acids, but differential modification for "M" and "C" were set at 15.994 and 57.000 Da, respectively). The output from SEQUEST search was filtered and compiled using PeptideProphet and ProteinProphet programs (26, 27). Our error rate of protein assignment is less than 1% as determined by comparing the proteomic data with six-frame translated *T. brucei* genomic sequence database that included 271,892 polypeptide entries STOP codon to-STOP codon (25). The data set presented here includes only the doubly tryptic peptides that have a minimum peptide identification probability of 0.9 and have a minimum SEQUEST X correlation value of 1.5 for +1 ions, 1.8 for +2 ions, and 2.5 for +3 ions. We excluded any peptide containing more than one missed trypsin cleavage site in the sequence. Proteins containing these peptides and with minimum identification probability of 0.9 were considered positive. All except one protein presented here was identified with two or more peptide matches and with a protein identification probability of ≥0.95. They all are unique proteins. For the protein identified with only one peptide match the MS/MS spectra and relevant scores are provided in supplemental Table S2 and supplemental Fig. S1.

Sequence Analysis—The probable functions of the proteins were assigned based on GeneDB annotation and for proteins with unknown function possible motifs and/or domains were searched in InterPro (http://www.ebi.ac.uk/Tools/InterProScan/), Pfam (http://pfam.sanger.ac.uk/) and NCBI CDD (http://www.ncbi.nlm.nih.gov/Structure/cdd/wrpsb.cgi) databases. The protein transmembrane topology was predicted using the TMHMM 2.0 program (http://www.cbs.dtu.dk/services/TMHMM).

Prediction of Protein-Protein Interactions—The composition of each complex was assessed by tagging multiple proteins individually as described above and by performing multiple MS analyses of each sample. The .out files (SEQUEST output) were compiled and filtered using the DTASelect program (28) to identify proteins in each analysis. Proteins identified with at least two tryptic peptides and with minimum peptide and protein identification probability of ≥0.9 were included in the list except for known non-mt proteins and highly abundant mt protein that are often seen in various TAP-tag experiments (17). The .raw files were converted to mzXML format and the Census program (29) was used to determine the spectral count of each of the peptides. For each individual protein, the number of spectra per peptide was calculated (sum of spectral count of all peptides respective to the protein/number of unique peptides). The relative ratio of spectra per peptide to bait protein (tagged protein) was calculated by dividing spectra per peptide value of each individual protein identified in the TAP-tag experiment by the spectra per peptide value of tagged protein. We used the Cytoscape software (http://www.cytoscape.org) to predict protein-protein interaction networks where a target protein was linked to bait protein if it had relative ratio of ≥1.0. A value of ≥1.25 was considered as high-confidence interactions.

RESULTS

In-gel Activity Staining of T. brucei mt Respiratory Complexes—Native electrophoresis and subsequent in-gel catalytic activity assays were used for visualization of respiratory chain complexes I–V (Figs. 1*A*–*C*). MS analyses were carried out on gel slices to assess the presence of the component protein(s) of complexes in the respective stained gel bands. Numerous proteins were identified in each gel slice (supplemental Table S1), some of which included known components of respiratory complexes. The large majority of the proteins that were detected are not part of the respective respiratory complexes, which likely reflects the complexity of the mt lysate samples and comigration of large complexes in native gels. However, some of these proteins, especially those with unknown functions, may be associated with their respective respiratory complexes.

NADH dehydrogenase activity revealed two stained bands (Fig. 1*A*). One band was in the well of the gel, suggesting that some material was not solubilized, very high molecular weight complexes and/or highly hydrophobic membrane-bound protein complexes that did not enter the gradient separation gel. The other band was observed at an apparent molecular weight of 1 MDa. MS analyses of the gel slice containing the ~1 MDa NADH dehydrogenase activity band predominantly identified Tb11.01.1740, Tb11.47.0004, Tb11.01.3550, and Tb11.01.8470 (supplemental Table S1), four proteins described as components of the 2-oxoglutarate dehydrogenase complex (OGDC) (16). Although the theoretical molecular mass of the bovine complex I was reported as 980 kDa (30),

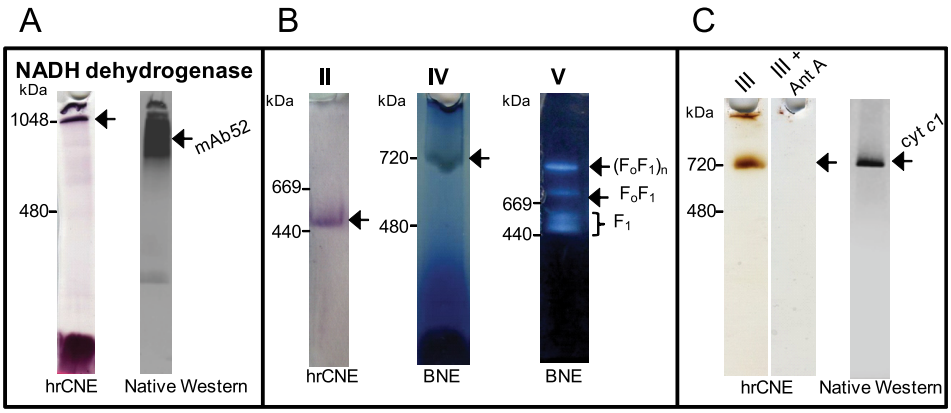

FIG. 1. **In-gel activity staining of *T. brucei* mt respiratory complexes separated by hrCNE and BNE.** Mt lysate was fractionated by hrCNE and BNE PAGE, and stained for (*A*) NADH dehydrogenase activity. The hrCNE gel was subsequently blotted and probed with mAb52, which recognizes a native epitope of the oxidoreductase complex (16). (*B*) Activity of complexes II, IV and V, and (*C*) activity of complex III in the absence and presence of antimycin A (Ant A). The hrCNE gel was also blotted and probed with polyclonal antibodies specific to the apoc$_1$ subunit of complex III. Arrows mark the major stained band in each case. The sizes of high molecular weight standards are indicated on the *left*.

only ten proteins out of the 30 nuclear-encoded subunits that were either predicted (31) or identified as part of the oxidoreductase complex (16, 25) were identified in this gel slice (supplemental Table S1, band 2). However, it was previously reported that *T. brucei* complex I has a mass of ~600 kDa (9, 32), thus we analyzed the entire lane of the native gel by MS including the well (supplemental Table S1, bands 1–10). MS analyses of the ~ 1 MDa to ~ 700 kDa region identified a total of 20 proteins out of the 30 subunits assigned to complex I (supplemental Table S1, bands 3 and 4). Western analysis using mAb52, which recognizes a native epitope in the oxidoreductase complex that corresponds to subcomplex Iα ((16) and this work) recognized the same region of the gel (Fig. 1*A*). These results suggest that NADH dehydrogenase activity staining reported earlier as complex I activity (9, 32) may not only be specific for complex I in PF cells, but it is also likely because of OGDC.

The complex II in-gel activity assay resembled the NADH dehydrogenase activity assay except that succinate rather than NADH was used as electron donor (Fig. 1*B*). MS analyses of the ~500 kDa reactive gel band identified Tb09.160.4380, Tb927.8.6580, and Tb927.8.3380, the three known core components of *T. brucei* SDH complex (supplemental Table S1), indicating that the stained band corresponds to *T. brucei* complex II. Specific in-gel complex IV staining revealed a band of an apparent molecular mass of ~ 700 kDa (Fig. 1*B*), and MS analyses identified 15 known subunits of complex IV (supplemental Table S1 and (17)). Complex V was stained by an ATP hydrolysis assay that can identify holo-F_oF_1 complex and catalytically active F_1 moiety as previously described in our study of *T. brucei* ATP synthase complex (Fig. 1*B* and (8)).

For the in-gel staining of complex III, we applied the method described previously for bovine heart complex III, in which 3,3′-diaminobenzidine tetrahydrochloride is used to stain complex III heme specifically (22). MS analyses of the gel slice containing the ~720 kDa activity band (Fig. 1*C*) identified two known subunits of complex III; Tb927.8.1890 and Tb09.211.4700 (supplemental Table S1). The specificity of the catalytic activity was further demonstrated by incubating the mt lysates with 2 mM antimycin A, a specific inhibitor of complex III before hrCNE electrophoresis (Fig. 1*C*). Upon inhibition with antimycin A, the ~720 kDa activity band was no longer visible, and only residual activities remained visible in the well, thus supporting that the stained band corresponds to complex III. Furthermore, native Western analysis with antibodies against apoc$_1$ (33), a core component of complex III, confirmed the size of the native complex III (Fig. 1*C*).

In summary, we visualized under native conditions the *T. brucei* mt respiratory complexes II–V by activity staining using the characteristic enzyme activities associated with each complex. The primary observed NADH dehydrogenase activity is most likely because of OGDC, however, *T. brucei* complex I was detected using a specific monoclonal antibody.

Identification of Mitochondrial-encoded Subunits of Respiratory Chain Complexes—The mt genome of *T. brucei*, like that of most other organisms, encodes subunits of the respiratory complexes, such as apocytochrome *b* (complex III), cytochrome *c* oxidase subunits I (COI), II (COII), and III (COIII), and subunit A6 of ATP synthase (34). To date, apocytochrome *b* and COI from *Leishmania tarentolae* are the only proteins identified that are translated from edited mRNAs (35–37), which are the processed RNA products of kinetoplastid mt DNA (kDNA). Liquid chromatography (LC)-MS/MS analyses of the ~1 MDa to ~700 kDa region (Fig. 1*A*) identified three unique peptides that match to the COII subunit of complex IV (Fig. 2 and supplemental Table S1) and COIII, another subunit of complex IV was identified by a single tryptic peptide in the gel slice containing the ~720 kDa activity band (Fig. 1*C*) (Fig. 2, supplemental Table S2 and supplemental Fig. S1). Fig. 2 shows the amino acid

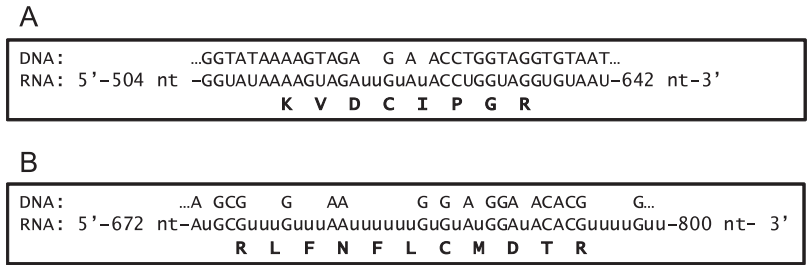

FIG. 2. **Identification of the mitochondrial encoded subunits COII and COIII.** A portion of the gene (DNA), edited mRNA (RNA) and amino acid sequence of the peptides identified by MS that match an edited region of (*A*) COII and of (*B*) COIII from *T. brucei*. The uridylate residues inserted by RNA editing are shown in lowercase. nt, nucleotide.

sequence of a tryptic peptide that matches the edited region of COII (Fig. 2*A*), and another peptide sequence that matches an edited region of COIII (Fig. 2*B*). Hence, peptides from two mt encoded-protein subunits of complex IV and their edited mRNAs were detected.

Tagged Respiratory Complexes—The data obtained by MS analyses from the gel slices as described above did not allow us to specifically determine the composition of complexes I–III. Therefore, we purified these complexes from *T. brucei* PF cells by tandem affinity purification (TAP) using two previously published methods (M1 and M2) (8, 16), and analyzed the protein composition by LC-MS/MS. The mt localization of almost all tagged proteins was confirmed by immunofluorescence analysis using anti-*myc* Ab (anti-tag), indicating that the tags as well as over-expression did not alter the mt localization (supplemental Fig. S2).

NADH Dehydrogenase Complex and Subunit Composition—Complex I is the largest and least understood complex of the respiratory chain. Mammalian complex I consists of ~46 different subunits that are assembled into a ~1 MDa structure. The subunit composition and general topology of complex I has been defined through its dissection into three subcomplexes (Iα + λ, Iβ, and Iγ) (38). The *T. brucei* genome database contains seven mt encoded and 12 nuclear encoded genes with homology to eukaryotic subunits (Table I). To purify complex I from *T. brucei*, Tb10.61.1790 (NDUFA6), Tb11.01.0640 (NDUFA13), Tb10.05.0070 (NDUFA9), Tb11.47.0017 (NDUFS7), Tb09.244.4620 (NDUFA9), and Tb10.70.3150 (NDUFA5) subunits of the subcomplex Iα + γ as well as Tb11.01.7460 (NDUFB9), a subunit of the subcomplex Iβ were tagged resulting in generation of TAP100, TAP205, TAP204, TAP206, TAP081, TAP203, and TAP157 cell lines, respectively (Table I). Unfortunately, we were not able to tag any subunits of subcomplex Iγ because it contains mt encoded subunits and methodology for expression of these subunits is not yet available. Purification of intact complex I was not observed potentially because of its instability during lysis and purification. MS analyses of the TAP100, TAP081, TAP203, and TAP157 purified complexes yielded two separate sets of proteins, of which many were annotated as hypothetical (supplemental Table S3). TAP204, TAP205, and TAP206 were not incorporated into the complex I because only the tagged proteins were identified by MS analyses (supplemental Table S3). Given that these proteins are predicted to be subunits of complex I (25, 31), most likely the tag interfered with the folding of the tagged protein or with its integration into the complex. To assess the validity of the association of the hypothetical [novel] proteins identified by MS analyses, three additional proteins associated with subcomplexes Iα + λ Tb927.2.4380 (TAP096), Tb09.160.5260 (TAP055 (16)), Tb927.7.7330 (TAP054), and one protein associated with subcomplex Iβ Tb11.01.7090 (TAP151) were also TAP-tagged. The SDS-PAGE of the subcomplexes Iα and Iβ (Figs. 3*A* and *B*) showed similar protein profiles for their respective subcomplexes, which differed mainly with respect to the abundance and position of the tagged bait as detected by Western blot analysis (data not shown). All of the most prominent gel bands in subcomplex Iα+λ were individually analyzed by MS and the respective proteins were identified (Fig. 3*A* and supplemental Table S3). Twenty four proteins were identified in this subcomplex. The most prominent bands in TAP151 purifications were also analyzed by MS and twelve proteins were identified in this subcomplex (Fig. 3B). These twelve proteins were also identified in TAP157 purification with the exception of NDUFAB1 and Tb09.160.0390 (supplemental Table S3). In addition, five other proteins were identified in at least two samples of the subcomplex Iα+λ (Tb11.01.8630, Tb10.70.3150, Tb09.244.2620, Tb927.1.730, Tb927.6.1410) and three more proteins (Tb11.01.7460, Tb11.02.2070, Tb927.8.5560) in subcomplex β when the SDS-PAGE step was omitted and samples were directly submitted to trypsin cleavage and LC-MS/MS analysis (supplemental Table S3).These proteins are most likely associated with the Iα+λ and β sub-complexes although their affinity of association and relative concentration (stoichiometry) may be lower compared with the proteins identified by gel-band analysis. These results suggest that subcomplexes Iα + γ and Iβ were purified, each subcomplex contains at least 32 and 15 subunits, respectively and they had no overlapping composition except for NDUFAB1 (Tb927.3.860) subunit, which was identified in both subcomplexes. All twelve nuclear-encoded proteins that have similarity to the eukaryotic complex I subunits as predicted by genome and proteome analysis (25, 31) have been identified in our TAP-tag complex purifications. However, we were not able to identify the seven mt encoded subunits ND1, ND3, ND4, ND5, ND7, ND8, and ND9 most likely because of their high hydrophobicity and properties such as few tryptic cleavage sites and

TABLE I

Trypanosoma brucei complex I subunits

√ indicates that only proteins identified in at least two experiments and by at least two unique tryptic peptides are shown. ND, protein has not been detected by MS. [TAP]Proteins used as baits.

Protein_Id[d]	Genome[f]/Proteome analysis[g]	Complex I Subcomplex Iα[h]	Complex I Subcomplex Iβ[i]	Domains/Motifs[e]	Homology with human/bovine proteins
Nuclear encoded					
Tb10.05.0070[TAP204]	√	√	ND	NADH-ubiquinone oxidoreductase complex I subunit	NDUFA9/39-kDa
Tb10.389.1140	√	√	ND	NADH-ubiquinone oxidoreductase, 75kDa 2Fe-2S ferredoxin-like	NDUFS1/75-kDa
Tb10.61.1790[TAP100]	√	√	ND	NADH-ubiquinone oxidoreductase, subunit B14	NDUFA6/B14
Tb11.01.0640[TAP205]	√	√	ND	NADH-ubiquinone oxidoreductase, subunit B16.6	NDUFA13/B16.6
Tb11.01.7460[TAP157]	√	ND	√	NADH-ubiquinone oxidoreductase, subunit NI2M	NDUFB9/B22
Tb11.01.8630	√	√	ND	NADH-ubiquinone oxidoreductase, subunit B8	NDUFA2/B8
Tb11.47.0017[TAP206]	√	√	ND	NADH-ubiquinone oxidoreductase, subunit NdhK	NDUFS7/PSST
Tb927.3.860	√	√	√	Acyl carrier protein	NDUFAB1/SDAP
Tb927.5.450	√	√	ND	NADH-ubiquinone oxidoreductase, 51 kDa	NDUFV1/51-kDa
Tb927.7.6350	√	√	ND	NADH-ubiquinone oxidoreductase, 24 kDa	NDUFV2/24-kDa
Tb09.160.0760	√	√	ND	Alpha/beta-Hydrolases	
[a]Tb09.160.5260[TAP055]	√	√	ND	2-enoyl thioester reductase	Trans-2-enoyl-CoA reductase
[a]Tb927.7.7410	√	√	ND	2-enoyl thioester reductase	Trans-2-enoyl-CoA reductase
Tb09.211.0330	√	√	ND	Heat shock protein DnaJ	DnaJ homolog
Tb09.244.2620[TAP081]	√	√	ND	NADB_Rossman super family, NDUFA9_like_SDR_a	
Tb09.244.2670	√	√	ND		
Tb10.6k15.3040	√	√	ND	Vacuolar H+-ATPase V1 sector, subunit C	
Tb10.70.3150[TAP203]	√	√	ND	NADH-ubiquinone oxidoreductase, 13 kDa-B subunit	NDUFA5/B13
Tb10.70.5510	√	√	ND	Adrenodoxin reductase, putative; ferredoxin	Adrenodoxin oxidoreductase; ferredoxin
Tb11.01.5480	√	√	ND		
[b]Tb11.01.7480	√	√	ND	Manganese and iron superoxide dismutase	Superoxide dismutase
[b]Tb927.5.3350	√	√	ND	Manganese and iron superoxide dismutase	Superoxide dismutase
Tb11.02.4810	√	√	ND	Phosphoenolpyruvate carboxykinase	
Tb927.1.730	√	√	ND	NB-ARC domain	
Tb927.2.4380[TAP096]	√	√	ND		
Tb927.3.3660	√	√	ND		
Tb927.6.1410	√	√	ND		
[c]Tb927.6.2010	√	√	ND	Acyl-CoA synthetase-like	Acyl-CoA synthetase
[c]Tb11.02.2070	√	ND	√	Acyl-CoA synthetase-like	Acyl-CoA synthetase
Tb927.7.7330[TAP054]	√	√	ND		
Tb927.8.4250	√	√	ND	Tetratricopeptide repeat	Tetratricopeptide repeat
Tb11.02.1020	√	√	ND		
Tb09.160.0390[g]	√	ND	√	Flavoprotein monooxygenase	Kynurenine 3-monooxygenase
Tb09.160.4910	√	ND	√	Flavoprotein monooxygenase	Kynurenine 3-monooxygenase
Tb09.211.1280	√	√	ND		
Tb09.211.2780	ND	ND	√		
Tb09.244.2840	√	ND	√		
Tb10.70.6930	√	ND	√		
Tb11.01.1690	√	ND	√		
Tb11.01.7090[TAP151]	√	ND	√	Complex1 LYR	LYR motif
Tb927.2.1680	√	√	ND	Cyclophilin-type peptidyl-prolyl cis-trans isomerase	Peptidyl-prolyl cis-trans isomerase
Tb927.4.4300	√	ND	√	SET domain	
Tb927.4.440	√	ND	√		
Tb927.7.3910	√	ND	√	P-loop containing nucleoside triphosphate hydrolases	
Tb927.8.2530	√	ND	√	Cytochrome C oxidase copper chaperone	

TABLE I—*continued*

Protein_Id[d]	Genome[f]/Proteome analysis[g]	Complex I Subcomplex Iα[h]	Complex I Subcomplex Iβ[i]	Domains/Motifs[e]	Homology with human/bovine proteins
Tb927.8.5560	√	ND	√	S-adenosyl-L-methionine-dependent methyltransferases	Methyltransferase
Mitochondrial encoded					
M94286	ND	ND	ND	36 kDa subunit 1	ND1/Chain1
AAA20887	ND	ND	ND	18 kDa CR5/G5 cryptogene	ND3/Chain3
AAB59224	ND	ND	ND	52 kDa subunit 4	ND4/Chain4
P04540	ND	ND	ND	71 kDa subunit 5	ND5/Chain5
P21301	ND	ND	ND	45 kDa 4Fe-FS protein	ND7/49kDa
gi 552291 gb AAA91499.1	ND	ND	ND	17 kDa subunit 8	ND8/TYKY
gi 162166 gb AAA03749.1	ND	ND	ND	14 kDa subunit 9	ND9/30kDa
Plant origin					
Tb11.02.5070	√	ND	ND	33 kDa plant 2	
Tb927.4.4980	ND	ND	ND	18 kDa plant 6	

[a, b, and c] Protein pairs with sequence homology.

[d] GeneDB accession number (http://www.genedb.org) or GeneBank (http://www.ncbi.nlm.nih.gov/GenBank/index.html) for the mitochondrially encoded polypeptides.

[e] All proteins have orthologs in *T. cruzi* and *L. major*.

[f] [31].

[g] [25] and native gel analysis (this study).

[h] Proteins identified in pull-downs with mAb 52, 63, 69 [16] and/or TAP054, TAP055 [16],TAP081,TAP096, TAP100, TAP203, TAP204, TAP205 and TAP206 affinity purification.

[i] Proteins identified in TAP151 and TAP157 affinity purification.

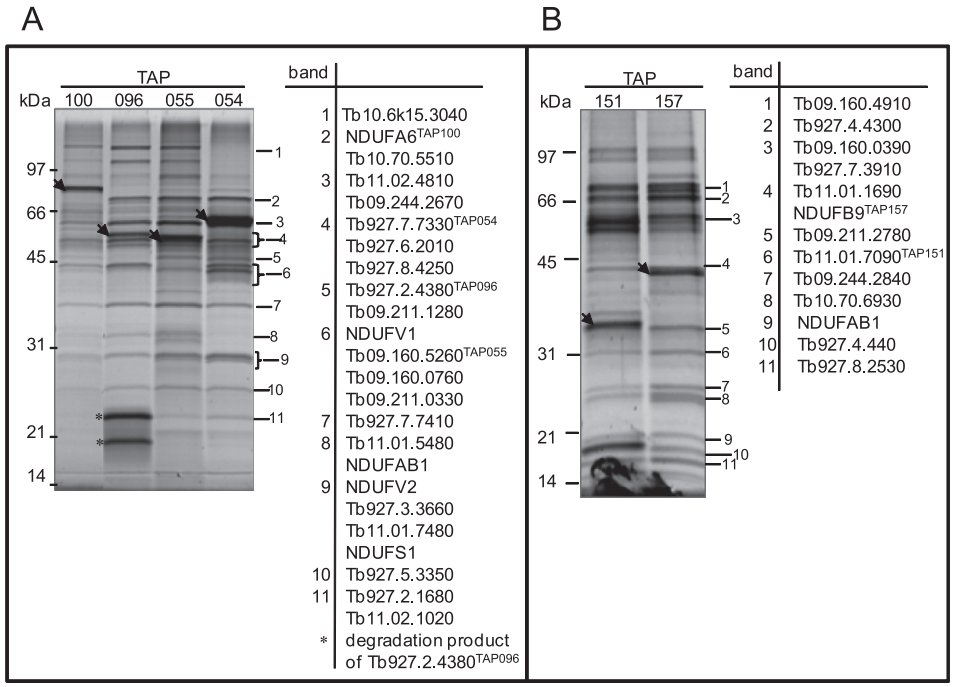

FIG. 3. **TAP tag purified *T. brucei* NADH:ubiquinone dehydrogenase complex.** *A*, TAP100, TAP096, TAP055 and TAP054 complexes were purified and separated on a 10–14.5% polyacrylamide Tris-glycine gel and stained with Sypro Ruby. The listed proteins were identified in the bands shown with corresponding numbers. The sizes of the protein marker are indicated. The position of tagged proteins is indicated by arrowheads. *B*, TAP151 and TAP157 complexes were purified and separated on a 10–14.5% and labeled as in A.

resulting cysteine rich peptides or not present in PFs (see discussion). Analysis of peptide sequences generated *in silico* indicated only six peptides has high probability of being detected by the MS approach taken in this study (data not shown). Also we were not able to identify in our purifications the two proteins that share identity with subunits of plant complex I ((31) and Table I), suggesting that these proteins may not be part of *T. brucei* complex I. Of all 46 proteins identified in purified complex I (subcomplexes I$\alpha+\lambda$ and Iβ combined), 24 are currently annotated as hypothetical in the GeneDB database. Several of the latter possess domains/motifs that are indicative of possible function(s) in oxidoreduc-

TABLE II

Trypanosoma brucei complex II subunits. Only proteins identified in at least two experiments and by at least two unique tryptic peptides are shown. [TAP]Proteins used as baits

Protein_ID[a]	Homolog/Domain[b]	Shotgun approach[c]	TAP Tag	Ortholog in T. cruzi[d]
Tb927.8.6580[TAP106]	SDH1	√	√	SDH1
Tb09.160.4380[TAP105]	$SDH2_C$	√	√	$SDH2_C$
Tb927.8.3380[TAP120]	$SDH2_N$	√	√	$SDH2_N$
Tb927.2.4700		√	√	SDH8
Tb927.8.5640		√	√	SDH6
Tb10.70.4500		√	√	SDH9
Tb927.6.4130		√	√	SDH3
Tb927.7.3590		√	√	
Tb927.8.1490	DUF1674 (domain of unknown function)	√	√	

[a] GeneDB accession number (http://www.genedb.org).
[b] All proteins have orthologs in *L. major*.
[c] [25] and native gel analysis (this study).
[d] [15].

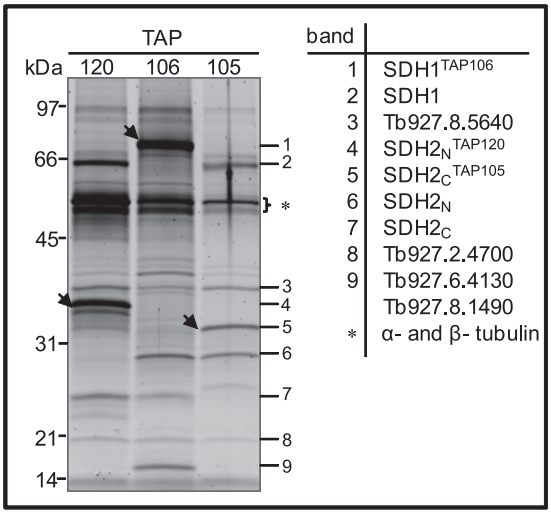

FIG. 4. **TAP tag purified *T. brucei* SDH Complex.** Sypro Ruby-stained SDS-PAGE protein profile of complexes, which were purified using TAP120, TAP106 and TAP105. The proteins identified by MS analysis of the corresponding band are shown and the position of tagged proteins is indicated by arrowheads. The asterisk indicates α- and β- tubulin.

tase processes (Table I). All together, we found that the *T. brucei* complex I is purified as two subcomplexes, and composed of at least 46 subunits (Table I).

SDH Complex and Subunit Composition—The large flavoprotein subunit Tb927.8.6580 (SDH1) and the smaller iron-sulfur subunit that is heterodimeric in Trypanosomatids (39) Tb927.8.3380, $SDH2_N$; Tb09.160.4380, $SDH2_C$ were tagged resulting in generation of TAP106, TAP120, and TAP105 cell lines (Table II). All visible gel bands (Fig. 4) were individually analyzed by MS and the respective proteins SDH1, $SDH2_N$, $SDH2_C$, and four hypothetical proteins Tb927.8.5640, Tb927.2.4700, Tb927.6.4130, and Tb927.8.1490, were identified in all three tagged complexes with at least two peptides (Fig. 4 and supplemental Table S4). In addition, two other proteins (Tb927.7.3590 and Tb10.70.4500) were identified in all three purifications when the SDS-PAGE step was omitted (supplemental Table S4).

In mammalian and bacterial mitochondria, SDH1 and SDH2 are anchored to the inner mt membrane by two small hydrophobic subunits, SDH3 and SDH4, which are required for electron transfer and ubiquinone reduction. These two subunits were not identified in the genome of the *T. brucei* by BLAST search suggesting that they may be highly diverged in sequence. However, two hypothetical proteins (Tb927.2.4700 and Tb927.7.3590) out of the nine proteins that were found associated with complex II possess predicted transmembrane domains and are similar in size to SDH3 and SDH4 (supplemental Table S4). This implies that they may play a role in electron transfer and perhaps function similar to SDH3 and SDH4 subunits, however direct comparison with these proteins did not reveal any predicted structural or motif similarity. In summary, we assigned nine proteins with high confidence to *T. brucei* SDH complex (Table II). This suggests that the complexity of the *T. brucei* complex is similar to that in *T. cruzi*, which is comprised of six hydrophobic and six hydrophilic subunits (15).

bc_1 Complex and Subunit Composition—In trypanosomatids, as in other eukaryotes, the bc_1 complex contains three subunits with active redox centers: the mt encoded cytochrome *b*, and the two nuclear encoded proteins, Tb927.8.1890 (cytochrome c_1) and the Rieske iron-sulfur protein (Tb09.211.4700, ISP). The latter two were tagged resulting in generation of TAP059 and TAP021 cell lines (Table III). Because the members of the mt processing peptidase family have been shown to be core subunits of complex III, as in yeast and mammals (40), Tb11.02.1480 the *T. brucei* homolog of the α-MMP was also tagged (TAP066). All visible gel bands (Fig. 5 and supplemental Table S5) were individually analyzed by MS and the respective proteins cytochrome c_1, ISP, α-MMP and Tb927.5.1060 (β-MMP) were identified in both purifications. Surprisingly, cytochrome c_1 was not detected by MS analysis in the purified TAP021 samples although,

TABLE III

Trypanosoma brucei complex III subunits. Only proteins identified in at least two experiments and by at least two unique tryptic peptides are shown. [TAP]Proteins used as baits

Protein_ID[a]	Homolog/Domain[b]	Shotgun approach[c]	TAP Tag
Nuclear encoded			
Tb09.211.4700[TAP021]	ISP	√	√
Tb927.8.1890[TAP059]	Cytochrome c_1	√	√
Tb11.02.1480[TAP066]	α-MMP	√	√
Tb927.5.1060	β-MMP	√	√
Tb10.70.2970[d]	Cytochrome bd ubiquinol oxidase, 14kDa subunit	√	√
Tb11.01.7900		√	√
Mitochondrial encoded			
AAA32115	apocytochrome *b*	ND	ND

[a] GeneDB accession number (http://www.genedb.org) or GeneBank (http://www.ncbi.nlm.nih.gov/GenBank/index.html) for the mitochondrially encoded polypeptide.

[b] All proteins have orthologs in *L. major* and in *T. cruzi*.

[c] [25] and native gel analysis (this study).

[d] Only identified in TAP066.

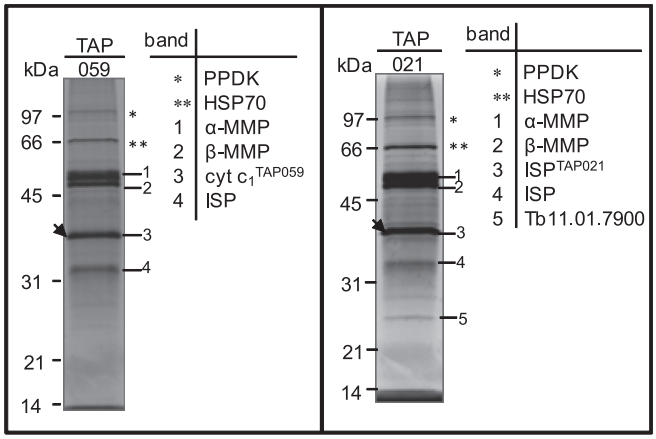

FIG. 5. **TAP tag purified *T. brucei* cytochrome bc_1 complex.** SYPRO Ruby-stained SDS-PAGE gels of TAP059 and TAP021 purifications. The proteins identified by MS analysis of the corresponding bands are indicated. The position of tagged proteins is indicated by arrowheads. PPDK, pyruvate phosphate dikinase; HSP70, heat shock 70 kDa protein.

detected when tagged itself (TAP059). Perhaps the TAP-tag interferes with the binding of cytochrome c_1 with ISP protein. The additional ISP band in TAP021 (Fig. 5) is probably a product of proteolysis of the tagged protein because two bands were also detected by Western blot analysis (data not shown). Tb11.01.7900 has been identified in gel band analysis in TAP021 and TAP066 purifications as well as in TAP059 purification when the SDS-PAGE step was omitted (Fig. 5 and supplemental Table S5). In addition, two other annotated hypothetical proteins (Tb11.01.8225 and Tb10.70.2970) were identified only in TAP066 purification (data not shown and supplemental Table S5). Although Tb10.70.2970 has been identified only in one TAP purification, we assigned it to complex III based on its ubiquinol-cytochrome *c* reductase domain and its 28% sequence identity to the *Saccharomyces cerevisiae* Qcr7p subunit, which has a role in the assembly of bc_1 complex (41). All together we were able to assign six proteins to the *T. brucei* complex III with high confidence (Table III).

Besides the respiratory complexes described above, *T. brucei* mitochondrion contains a branched electron transport chain that is composed of the mt FAD-linked glycerol-3-phosphate dehydrogenase (Tb927.1.1130) and alternative oxidase TAO (Tb10.6k15.3640) (Fig. 6*A*). Moreover, an alternative rotenone-insensitive NADH dehydrogenase (Tb10.6k15.0960), which also occurs in plants and fungi, was characterized in *T. brucei* cells (42). All three enzymes are predicted to work as single proteins; however, these predictions have not been experimentally verified. Thus, all three proteins were tagged resulting in TAP208, TAP207, and TAP210 cell lines respectively, and TAP-purified samples were then subjected to SDS-PAGE fractionation and to LC-MS/MS analyses (Fig. 6*B*). SyproRuby-stained gel and MS data showed that alternative dehydrogenase and glycerol-3-phosphate dehydrogenase were purified as single protein since except typical contamination arising from α- and β-tubulin, only the bait protein was identified by MS. In TAP207 two protein bands were apparent on SDS-PAGE gel (Fig. 6*B*), the higher one corresponding to the tagged version of the TAO and the second one representing the endogenous protein, suggesting that this enzyme exists as a dimer or multimer.

Protein-Protein Interaction Map—The acquired MS data from TAP-tag purified multiprotein complexes was used to predict a protein-protein interaction network of the respiratome (Fig. 7). The bold lines in Fig. 7 indicate high confidence predicted direct-interactions between the indicated proteins, and dotted lines indicate additional proteins pulled-down by the bait (tagged protein). As described above, complex I exists as multiple subunits, and results from the interaction map suggest Tb927.3.860 (NDUFAB1) interacts with Tb11.01.7090 and connects subcomplex Iα and Iβ. Six addi-

A

GeneDB ID	Annotation	TAP
Tb10.6k15.3640	Alternative oxidase (TAO)	207
Tb10.6k15.0960	Alternative dehydrogenase	210
Tb927.1.1130	Glycerol-3-phosphate dehydrogenase	208

B

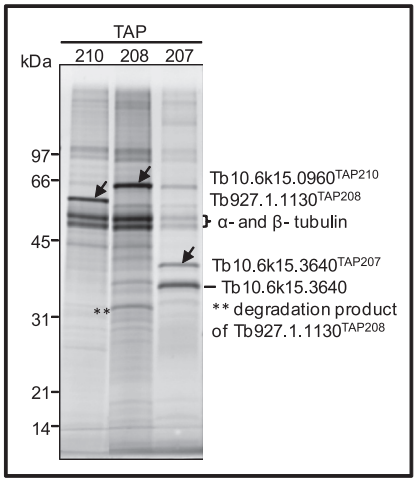

FIG. 6. **TAP tag purified *T. brucei* glycerol-3-phosphate dehydrogenase, alternative dehydrogenase and alternative oxidase.** *A*, Annotated and tagged enzymes. *B*, Sypro Ruby staining of TAP-tag purified proteins. The arrowheads indicate the tagged proteins that were identified by MS analysis. The sizes of the protein marker are indicated on *left*.

tional proteins (Tb10.70.1520, Tb11.02.0290, Tb10.v4.0045, Tb09.211.1600, Tb927.8.6960, and Tb927.5.3300) with unknown function were identified in complex I map that did not match our criteria of being identified in two separate TAP-tag experiments (Fig. 7), thus they are not included as bona-fide components of complex I in Table I. However, these are possible components of complex I or other complex(es) that may associate with complex I. Similarly, a number of proteins that did not match our criteria were identified in complex III, IV, and V map (Fig. 7). We also identified two components of complex III (Tb09.211.4700 and Tb11.01.7900) in purified subcomplex Iα. Similarly, four components of complex V (Tb927.7.7420/7430, α; Tb927.3.1380, β; Tb10.100.0070, γ; and Tb11.02.4120) were identified in complex IV preparation, and a potential new component of complex V Tb927.2.5930 was identified by this analysis as we included additional TAP-tag data than published earlier (8). We also found "MIX" protein (Tb927.5.3040) associated with components of complex IV, which we previously reported (17). These results identify the possible linking partners between the five respiratory complexes. However, the interactions have not yet been identified from genuine reciprocal interactions between the different subunits, thus further experimental evidence is required for validating these predictions especially as spurious association of proteins or highly abundant mt proteins may result in erroneous prediction. Overall, aggregate data may be useful for identifying component compositions of multi-protein complexes, where data from multiple TAP-tags and multiple MS runs are available.

DISCUSSION

The composition of the respiratory complexes was explored using native gel electrophoresis combined with in-gel activity staining, Western blot analysis and TAP-tag complex purification coupled with MS analysis. Respiratory complexes I, II, and III were purified using multiple tagged subunits and protein assignments were made based on the results from several purifications. In addition, the aggregate spectral counts of identified peptides from the TAP-tag studies were used to generate a preliminary protein-protein interaction map of the respiratory complexes. The interactions are consistent with the known structure of the respiratory complexes, *e.g.* complex I organized in subcomplexes, association of "MIX" protein with complex IV (17).The interaction map is consistent with our finding that RNAi knockdown of Tb10.70.7760 in complex V, resulted in the loss of the F_oF_1 complex interactions that contains the interactor, but the F_1 moiety was retained (8). Also, we report the first evidence of MS identification of mt proteins encoded by edited RNAs in *T. brucei*. Two tryptic peptides match edited region of COII and COIII, indicating that translated products from fully edited mRNA were detected. The results suggest that electrophoresis under native conditions might avoid the loss of these highly hydrophobic subunits, which have a tendency to aggregate and precipitate when in SDS (13, 33).

Successful activity staining of the respiratory complex II and III helped to estimate the native size of these complexes which range from ~450 to ~720 kDa. Complex II is an integral membrane protein complex involved in both the Krebs cycle and the respiratory electron transport chain. The total molecular mass of SDH complex is calculated to be ~220 kDa if it contained equimolar amounts of subunits. However, the activity band detected in hrCNE gel runs at ~450 kDa which may suggest that complex II exists as a homodimer. It is also possible that the complex is a monomer but migrates at a higher size in native gel because of the effect of salt, detergent etc. Nevertheless dimeric complex II has been reported for *T. cruzi* (15). Among the 12 subunits that compose *T. cruzi* complex II, our TAP tag analyses did not identify the ortholog of SDH4, SDH5 and SDH11, whereas we identified two other subunits of *T. brucei* complex II that are not present in the *T. cruzi* complex (Table II). Moreover, we identified the ortholog of SDH7 and SDH10 but they did not match our criteria of being identified in two separate TAP-tag experiments and/or by more than one peptide (supplemental Table S4). The homologs of the membrane bound subunits SDH3 and SDH4 are difficult to identify with conventional BLAST programs due to their highly diverged sequence. However, their putative homologs were identified in *T. cruzi* purified complex II based on the presence of quinone/heme binding motifs (15). The ortholog of *T. cruzi* SDH3 was identified in our preparation,

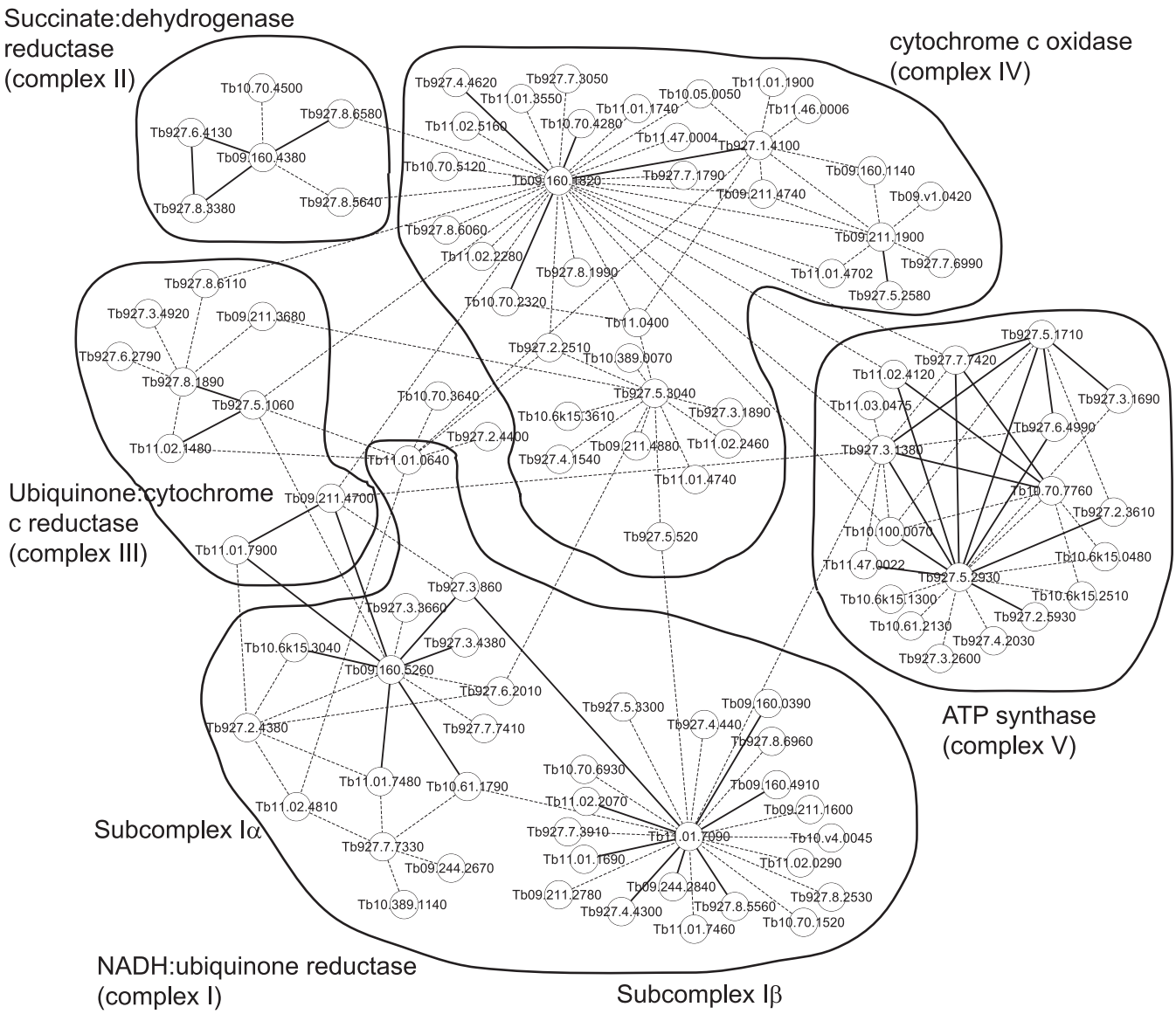

FIG. 7. **Predicted protein-protein interaction network of the *T. brucei* respiratome.** This Cytoscape graphical representation shows probable interactions within each respiratory complexes I-V and within the respiratome. The bold line indicates high confidence potential direct-interaction between the indicated proteins, and dotted line indicates additional proteins that were pulled-down by the bait.

but it appears that this protein (Tb927.6.4130) does not have a predicted transmembrane domain in *T. brucei* (supplemental Table S4). The supramolecular organization of *T. brucei* complex II resembles the *T. cruzi* complex, but is divergent from the *S. cerevisiae* and mammalian SDH complex structure, indicating that trypanosomatid SDH complex contains additional non-catalytic subunits as it was previously suggested for plant complex II (43).

In *S. cerevisiae*, mutation in any one of the four genes leads to the loss of complex II function and the inability of *S. cerevisiae* to grow by respiration (reviewed in (44)). In contrast, *T. brucei* RNAi knockdown of the core subunits of complex II resulted in a complete loss of oxidative phosphorylation in response to succinate, but were conditionally lethal only in the absence of glucose (45, 46). Our functional analysis of the core subunits by RNAi showed that the complex II is not essential for the growth of *T. brucei* cells even in the absence of glucose (supplemental Fig. S3 and data not shown). These results suggest that *Trypanosoma* complex II is not the main entrance for electrons into the respiratory chain in PF cells.

bc_1 complex (complex III) is typically a structurally dimeric protein complex. In yeast and in bovine mitochondria, it exists in association with one and two copies of complex IV (47, 48). The total mass of the six proteins identified in this study is 237 kDa (supplemental Table S5), but it migrates at ~720 kDa indicating that *T. brucei* complex III could similarly form a multimer. The same size band (~720kDa) is observed for

cytochrome *c* oxidase activity, which has a predicted monomer size of ~360 kDa (17). Hence, the stained band may correspond to the bc_1-cytochrome *c* oxidase heteromultimeric-supercomplex as described in yeast (48). A bc_1-cytochrome *c* oxidase supercomplex is also suggested by MS analyses of the ~720 kDa activity band that revealed five core components of complex IV (supplemental Table 1). Nevertheless, this possible association does not appear to be essential for the structural integrity of either complex because repression of components of either complex that result in the loss of one complex do not result in the loss of the other complex (9).

Purified complexes III from *Crithidia fasciculate* (13, 33) and *L. tarentolae* (14) consist of ten and eleven subunits, respectively. Whereas only six subunits were found in the complex purified from *T. brucei*. This suggests a differential composition of complex III among trypanosomatids, or nonspecific association of other proteins with *Leishmania* and *Crithidia* complexes. It is also possible that the protein components identified in TAP purified complex III in this analysis are the more stably associated proteins. Other proteins that correspond to those seen in the other species may not be stably associated with the complex, but may have similar functions *in vivo*.

Although hrCNE combined with NADH:NTB reductase was successfully applied for the detection of bovine complex I (22), we found that the *T. brucei* NADH dehydrogenase activity stained band corresponded primarily to OGDC. In *T. brucei*, dihydrolipoyl dehydrogenase, one of the four subunits of OGDC is shared between OGDC and the pyruvate dehydrogenase complex (16). Its activity was detected using the same approach in mammalian mitochondria, implying that this assay is not specific for complex I activity (49). Furthermore, using a nongradient BNE method, both complex I and dihydrolipoyl dehydrogenase protein were detected simultaneously on the same gel (50), suggesting that the gel-based method used to separate mt respiratory complexes could be critical. Moreover, *Trypanosoma* subcomplex Iα and OGDC cosediment in glycerol gradients (16), implying that the native size of both complexes might be very similar and their respective activities may overlap in native gel. However, MS analysis revealed the presence of OGDC rather than *T. brucei* complex I in the NADH activity band, suggesting that the activity of complex I cannot be readily detected in this system. These results may imply that complex I has a limited activity and role in NADH reoxidation in culture-grown PF cells. This assumption is further supported by a novel finding that complex I is not essential for the growth of PF cells (51). Thus it is plausible to hypothesize that most of the mitochondrially generated NADH is regenerated in PFs by an alternative dehydrogenase which is also localized in the inner membrane (52). In addition, it has been reported that deletions in the ND4, ND5, and ND7 genes that encode for complex I mt subunits occurring in natural mutants of *T. cruzi* have no consequence to the mt redox state, indicating that complex I can have limited function in NADH oxidation in this species (53).

In general, complex I is composed of 14 subunits in prokaryotes and up to 46 subunits in eukaryotes. Yet, only 19 subunits of *Trypanosoma* complex I were found to have some degree of homology to these subunits based on homology search (25, 31). Out of these 19 subunits, all 12 nuclear-encoded ones were identified in our purified complexes, however none of the seven mt encoded subunits were detected by MS possibly due to the characteristics of these proteins, making their peptide identification by routine mass spectrometry analysis difficult. Moreover, some of these subunits may be present at very low abundance/absent in PF as they are preferentially edited in BF cells (54).

Previous purification of the hydrophilic subcomplex I$\alpha+\lambda$ of complex I suggested that *T. brucei* complex I is a unique multifunctional complex in trypanosomes that is involved not only in respiration but also in fatty acid synthesis (16). Our high confidence interaction map (Fig. 7) shows Tb11.02.2070, a long-chain-fatty acid-CoA ligase protein to be associated with subcomplex Iβ. In addition, the acyl carrier protein (NDUFAB1) that links subcomplex Iα with Iβ has homology to two acyl carrier proteins (ACPM1 and ACPM2) of *Yarrowia lipolytica*, which play roles in mitochondrial fatty acid metabolism as well as complex I assembly (55). Two flavoprotein monooxygenases were also identified as subunits of complex I. The members of the flavoprotein monooxygenases are usually involved in the microbial degradation of aromatic compounds, in biosynthesis of ubiquinone, and in detoxification of drugs and other xenobiotics (56). Thus, presence of such proteins reinforce that the complex I in trypanosomes is multifunctional.

Overall, this study characterized the composition of respiratory complexes I, II and III, identified not only the predicted subunits but also novel complex-associated proteins. These results expand our knowledge of the unique mt respiratory machinery in these early diverged parasitic protozoa. We also created a protein-protein interaction network of the respiratome. Although, we have not validated our prediction network, it provides a framework and candidates for downstream analyses.

Acknowledgments—We thank Yuko Ogata for help with mass spectrometry; Steve L. Hajduk (University of Georgia, Athens) for the apoc_1 antibody.

* This work was supported by National Institutes of Health grant AI065935 to KS. AZ received support from grant 204/09/P563 from the Grant Agency of the Czech Republic. Research was conducted using equipment made possible by support from the Economic Development Administration - US Department of Commerce and the M.J. Murdock Charitable Trust.

** These authors contributed equally to this work.

[S] This article contains supplemental Figs. S1 to S3 and Tables S1 to S5.

‖ To whom correspondence should be addressed: Seattle Biomedical Research Institute, 307 Westlake Ave N, Suite 500, Seattle, WA 98109-5219. Tel.: +1 206-256-7316; Fax: +1 206-256-7229; E-mail: ken.stuart@seattlebiomed.org.

REFERENCES

1. von Ballmoos, C., Cook, G. M., and Dimroth, P. (2008) Unique rotary ATP synthase and its biological diversity. *Annu. Rev. Biophys.* **37,** 43–64
2. Tielens, A. G., Rotte, C., van Hellemond, J. J., and Martin, W. (2002) Mitochondria as we don't know them. *Trends Biochem. Sci.* **27,** 564–572
3. Tielens, A. G., and van Hellemond, J. J. (2009) Surprising variety in energy metabolism within Trypanosomatidae. *Trends Parasitol.* **25,** 482–490
4. Vickerman, K. (1985) Developmental cycles and biology of pathogenic trypanosomes. *Br. Med. Bull.* **41,** 105–114
5. Bienen, E. J., Maturi, R. K., Pollakis, G., and Clarkson, A. B., Jr. (1993) Non-cytochrome mediated mitochondrial ATP production in bloodstream form *Trypanosoma brucei brucei. Eur. J. Biochem.* **216,** 75–80
6. Chaudhuri, M., Ott, R. D., and Hill, G. C. (2006) Trypanosome alternative oxidase: from molecule to function. *Trends Parasitol.* **22,** 484–491
7. Schnaufer, A., Clark-Walker, G. D., Steinberg, A. G., and Stuart, K. (2005) The F(1)-ATP synthase complex in bloodstream stage trypanosomes has an unusual and essential function. *EMBO J.* **24,** 4029–4040
8. Ziková, A., Schnaufer, A., Dalley, R. A., Panigrahi, A. K., and Stuart, K. D. (2009) The F(0)F(1)-ATP synthase complex contains novel subunits and is essential for procyclic *Trypanosoma brucei. PLoS Pathog.* **5,** e1000436
9. Horváth, A., Horakova, E., Dunajciková, P., Verner, Z., Pravdová, E., Slapetová, I., Cuninková, L., and Lukes, J. (2005) Downregulation of the nuclear-encoded subunits of the complexes III and IV disrupts their respective complexes but not complex I in procyclic *Trypanosoma brucei. Mol. Microbiol.* **58,** 116–130
10. Besteiro, S., Barrett, M. P., Rivière, L., and Bringaud, F. (2005) Energy generation in insect stages of *Trypanosoma brucei:* metabolism in flux. *Trends Parasitol.* **21,** 185–191
11. Berriman, M., Ghedin, E., Hertz-Fowler, C., Blandin, G., Lennard, N. J., Renauld, H., Bartholomeu, D., Caler, E., Hamlin, N., Haas, B., Böhme, U., Harris, B. R., Hannick, L., Barrell, B., Donelson, J., Hall, N., Fraser, C. M., Melville, S. E., El-Sayed, N., Shallom, J., Aslett, M., Hou, L., Atkin, B., Barron, A. J., Bringaud, F., Brooks, K., Cherevach, I., Chillingworth, T., Churcher, C., Clark, L. N., Corton, C. H., Cronin, A., Davies, R., Doggett, J., Djikeng, A., Feldblyum, T., Fraser, A., Goodhead, I., Hance, Z., Harper, A. D., Hauser, H., Hostetler, J., Jagels, K., Johnson, D., Johnson, J., Jones, C., Kerhornou, A., Koo, H., Larke, N., Larkin, C., Leech, V., Line, A., MacLeod, A., Mooney, P., Moule, S., Mungall, K., Norbertczak, H., Ormond, D., Pai, G., Peterson, J., Quail, M. A., Rajandream, M. A., Reitter, C., Sanders, M., Schobel, S., Sharp, S., Simmonds, M., Simpson, A. J., Tallon, L., Turner, C. M., Tait, A., Tivey, A., Van Aken, S., Walker, D., Wanless, D., White, B., White, O., Whitehead, S., Wortman, J., Barry, J. D., Fairlamb, A. H., Field, M. C., Gull, K., Landfear, S., Marcello, L., Martin, D. M., Opperdoes, F., Ullu, E., Whickstead, B., Alsmark, C., Arrowsmith, C., Carrington, M., Embley, T. M., Ivens, A., Lord, A., Morgan, G. M., Peacock, C. S., Rabbinowitsch, E., Salzberg, S., Wang, S., Woodward, J., and Adams, M. D. (2005) The genome of the African trypanosome, *Trypanosoma brucei. Science* **309,** 416–422
12. Speijer, D., Muijsers, A. O., Dekker, H., de, Haan, A., Breek, C. K., Albracht, S. P., and Benne, R. (1996) Purification and characterization of cytochrome c oxidase from the insect trypanosomatid *Crithidia fasciculata. Mol. Biochem. Parasitol.* **79,** 47–59
13. Speijer, D., Breek, C. K., Muijsers, A. O., Hartog, A. F., Berden, J. A., Albracht, S. P., Samyn, B., Van Beeumen, J., and Benne, R. (1997) Characterization of the respiratory chain from cultured *Crithidia fasciculata. Mol. Biochem. Parasitol.* **85,** 171–186
14. Horváth, A., Berry, E. A., Huang, L. S., and Maslov, D. A. (2000) Leishmania tarentolae: a parallel isolation of cytochrome bc(1) and cytochrome c oxidase. *Exp. Parasitol.* **96,** 160–167
15. Morales, J., Mogi, T., Mineki, S., Takashima, E., Mineki, R., Hirawake, H., Sakamoto, K., Omura, S., and Kita, K. (2009) Novel mitochondrial complex II isolated from *Trypanosoma cruzi* is composed of 12 peptides including a heterodimeric Ip subunit. *J. Biol. Chem.* **284,** 7255–7263
16. Panigrahi, A. K., Ziková, A., Dalley, R. A., Acestor, N., Ogata, Y., Anupama, A., Myler, P. J., and Stuart, K. D. (2008) Mitochondrial complexes in *Trypanosoma brucei*: a novel complex and a unique oxidoreductase complex. *Mol. Cell. Proteomics* **7,** 534–545
17. Ziková, A., Panigrahi, A. K., Uboldi, A. D., Dalley, R. A., Handman, E., and Stuart, K. (2008) Structural and functional association of *Trypanosoma brucei* MIX protein with cytochrome c oxidase complex. *Eukaryot Cell* **7,** 1994–2003
18. Wirtz, E., Leal, S., Ochatt, C., and Cross, G. A. M. (1999) A tightly regulated inducible expression system for conditional gene knock-outs and dominant-negative genetics in *Trypanosoma brucei. Mol. Biochem. Parasitol.* **99,** 89–101
19. Jensen, B. C., Kifer, C. T., Brekken, D. L., Randall, A. C., Wang, Q., Drees, B. L., and Parsons, M. (2007) Characterization of protein kinase CK2 from *Trypanosoma brucei. Mol. Biochem. Parasitol.* **151,** 28–40
20. Panigrahi, A. K., Schnaufer, A., Ernst, N. L., Wang, B., Carmean, N., Salavati, R., and Stuart, K. (2003) Identification of novel components of *Trypanosoma brucei* editosomes. *RNA.* **9,** 484–492
21. Panigrahi, A. K., Schnaufer, A., and Stuart, K. D. (2007) Isolation and Compositional Analysis of Trypanosomatid Editosomes, In: Gott, J. M. (ed), *Methods in Enzymology*, Vol 424 Ed., pp. 3–24, Elsevier Inc.
22. Wittig, I., Karas, M., and Schägger, H. (2007) High resolution clear native electrophoresis for in-gel functional assays and fluorescence studies of membrane protein complexes. *Mol. Cell Proteomics.* **6,** 1215–1225
23. Priest, J. W., and Hajduk, S. L. (2003) Trypanosoma brucei cytochrome c1 is imported into mitochondria along an unusual pathway. *J. Biol. Chem.* **278,** 15084–15094
24. Ziková, A., Panigrahi, A. K., Dalley, R. A., Acestor, N., Anupama, A., Ogata, Y., Myler, P. J., and Stuart, K. (2008) Trypanosoma brucei mitochondrial ribosomes: affinity purification and component identification by mass spectrometry. *Mol. Cell Proteomics* **7,** 1286–1296
25. Panigrahi, A. K., Ogata, Y., Ziková, A., Anupama, A., Dalley, R. A., Acestor, N., Myler, P. J., and Stuart, K. D. (2009) A comprehensive analysis of *Trypanosoma brucei* mitochondrial proteome. *Proteomics* **9,** 434–450
26. Keller, A., Nesvizhskii, A. I., Kolker, E., and Aebersold, R. (2002) Empirical statistical model to estimate the accuracy of peptide identifications made by MS/MS and database search. *Anal. Chem.* **74,** 5383–5392
27. Nesvizhskii, A. I., Keller, A., Kolker, E., and Aebersold, R. (2003) A statistical model for identifying proteins by tandem mass spectrometry. *Anal. Chem.* **75,** 4646–4658
28. Tabb, D. L., McDonald, W. H., and Yates, J. R., 3rd (2002) DTASelect and Contrast: tools for assembling and comparing protein identifications from shotgun proteomics. *J Proteome. Res.* **1,** 21–26
29. Park, S. K., Venable, J. D., Xu, T., and Yates, J. R., 3rd (2008) A quantitative analysis software tool for mass spectrometry-based proteomics. *Nat Methods.* **5,** 319–322
30. Carroll, J., Fearnley, I. M., Shannon, R. J., Hirst, J., and Walker, J. E. (2003) Analysis of the subunit composition of complex I from bovine heart mitochondria. *Mol Cell Proteomics.* **2,** 117–126
31. Opperdoes, F. R., and Michels, P. A. (2008) Complex I of Trypanosomatidae: does it exist? *Trends Parasitol.* **24,** 310–317
32. Fang, J., Wang, Y., and Beattie, D. S. (2001) Isolation and characterization of complex I, rotenone-sensitive NADH: ubiquinone oxidoreductase, from the procyclic forms of *Trypanosoma brucei. Eur. J. Biochem.* **268,** 3075–3082
33. Priest, J. W., and Hajduk, S. L. (1992) Cytochrome *c* reductase purified from *Crithidia fasciculata* contains an atypical cytochrome c_1. *J. Biol. Chem.* **267,** 20188–20195
34. Stuart, K., and Feagin, J. E. (1992) Mitochondrial DNA of kinetoplastids. *Int. Rev. Cytol.* **141,** 65–88
35. Horváth, A., Berry, E. A., and Maslov, D. A. (2000) Translation of the edited mRNA for cytochrome b in trypanosome mitochondria. *Science.* **287,** 1639–1640
36. Horvath, A., Kingan, T. G., and Maslov, D. A. (2000) Detection of the mitochondrially encoded cytochrome c oxidase subunit I in the trypanosomatid protozoan *Leishmania tarentolae. Evidence for translation of unedited mRNA in the kinetoplast. J. Biol. Chem.* **275,** 17160–17165
37. Hashimi, H., Benkovicová, V., Cermaková, P., Lai, D. H., Horváth, A., and Lukes, J. (2010) The assembly of F(1)F(O)-ATP synthase is disrupted upon interference of RNA editing in *Trypanosoma brucei. Int. J Parasitol.* **40,** 45–54
38. Lazarou, M., Thorburn, D. R., Ryan, M. T., and McKenzie, M. (2009) Assembly of mitochondrial complex I and defects in disease. *Biochim. Biophys. Acta* **1793,** 78–88

39. Gawryluk, R. M., and Gray, M. W. A split and rearranged nuclear gene encoding the iron-sulfur subunit of mitochondrial succinate dehydrogenase in Euglenozoa. *BMC Res. Notes.* 2: 16:16, 2009
40. Iwata, S., Lee, J. W., Okada, K., Lee, J. K., Iwata, M., Rasmussen, B., Link, T. A., Ramaswamy, S., and Jap, B. K. (1998) Complete structure of the 11-subunit bovine mitochondrial cytochrome bc1 complex. *Science* **281,** 64–71
41. Hemrika, W., De, Jong, M., Berden, J. A., and Grivell, L. A. (1994) The C-terminus of the 14-kDa subunit of ubiquinol-cytochrome-c oxidoreductase of the yeast *Saccharomyces cerevisiae* is involved in the assembly of a functional enzyme. *Eur. J Biochem.* **220,** 569–576
42. Fang, J., and Beattie, D. S. (2002) Novel FMN-containing rotenone-insensitive NADH dehydrogenase from *Trypanosoma brucei* mitochondria: isolation and characterization. *Biochemistry* **41,** 3065–3072
43. Millar, A. H., Eubel, H., Jänsch, L., Kruft, V., Heazlewood, J. L., and Braun, H. P. (2004) Mitochondrial cytochrome c oxidase and succinate dehydrogenase complexes contain plant specific subunits. *Plant Mol. Biol.* **56,** 77–90
44. Lemire, B. D., and Oyedotun, K. S. (2002) The *Saccharomyces cerevisiae* mitochondrial succinate:ubiquinone oxidoreductase. *Biochim. Biophys. Acta* **1553,** 102–116
45. Bochud-Allemann, N., and Schneider, A. (2002) Mitochondrial substrate level phosphorylation is essential for growth of procyclic *Trypanosoma brucei. J. Biol. Chem.* **277,** 32849–32854
46. Coustou, V., Biran, M., Breton, M., Guegan, F., Rivière, L., Plazolles, N., Nolan, D., Barrett, M. P., Franconi, J. M., and Bringaud, F. (2008) Glucose-induced remodeling of intermediary and energy metabolism in procyclic *Trypanosoma brucei. J. Biol. Chem.* **283,** 16342–16354
47. Schägger, H., and Pfeiffer, K. (2000) Supercomplexes in the respiratory chains of yeast and mammalian mitochondria. *EMBO J.* **19,** 1777–1783
48. Cruciat, C. M., Brunner, S., Baumann, F., Neupert, W., and Stuart, R. A. (2000) The cytochrome bc1 and cytochrome c oxidase complexes associate to form a single supracomplex in yeast mitochondria. *J. Biol. Chem.* **275,** 18093–18098
49. Yan, L. J., Yang, S. H., Shu, H., Prokai, L., and Forster, M. J. (2007) Histochemical staining and quantification of dihydrolipoamide dehydrogenase diaphorase activity using blue native PAGE. *Electrophoresis* **28,** 1036–1045
50. Yan, L. J., and Forster, M. J. (2009) Resolving mitochondrial protein complexes using nongradient blue native polyacrylamide gel electrophoresis. *Anal. Biochem.* **389,** 143–149
51. Verner, Z., Cermakova, P., Skodova, I., Kriegova, E., Horvath, A., and Lukes, J. (2010) Complex I (NADH:ubiquinone oxidoreductase) is active in but non-essential for procyclic *Trypanosoma brucei. Mol. Biochem. Parasitol.* doi:10.1016/j.molbiopara.2010.11.003
52. Fang, J., and Beattie, D. S. (2003) Alternative oxidase present in procyclic *Trypanosoma brucei* may act to lower the mitochondrial production of superoxide. *Arch. Biochem. Biophys.* **414,** 294–302
53. Carranza, J. C., Kowaltowski, A. J., Mendonca, M. A., de Oliveira, T. C., Gadelha, F. R., and Zingales, B. (2009) Mitochondrial bioenergetics and redox state are unaltered in *Trypanosoma cruzi* isolates with compromised mitochondrial complex I subunit genes. *J. Bioenerg. Biomembr.* **41,** 299–308
54. Corell, R. A., Myler, P. J., and Stuart, K. (1994) Trypanosoma brucei mitochondrial gene CR4 encodes an extensively edited mRNA with completely edited sequence only in the bloodstream forms. *Mol. Biochem. Parasitol.* **64,** 65–74
55. Dobrynin, K., Abdrakhmanova, A., Richers, S., Hunte, C., Kerscher, S., and Brandt, U. (2010) Characterization of two different acyl carrier proteins in complex I from *Yarrowia lipolytica. Biochim. Biophys Acta* **1797,** 152–159
56. van Berkel, W. J., Kamerbeek, N. M., and Fraaije, M. W. (2006) Flavoprotein monooxygenases, a diverse class of oxidative biocatalysts. *J. Biotechnol.* **124,** 670–689